

Tracking of coordinated groups using marginalised MCMC-based Particle algorithm

François Septier, Sze Kim Pang, Simon Godsill, Avishy Carmi

► **To cite this version:**

François Septier, Sze Kim Pang, Simon Godsill, Avishy Carmi. Tracking of coordinated groups using marginalised MCMC-based Particle algorithm. IEEE Aerospace Conference, Mar 2009, Big Sky, MT, United States. pp.1, 2009, <10.1109/AERO.2009.4839491>. <hal-00566621>

HAL Id: hal-00566621

<https://hal-imt.archives-ouvertes.fr/hal-00566621>

Submitted on 16 Apr 2013

HAL is a multi-disciplinary open access archive for the deposit and dissemination of scientific research documents, whether they are published or not. The documents may come from teaching and research institutions in France or abroad, or from public or private research centers.

L'archive ouverte pluridisciplinaire **HAL**, est destinée au dépôt et à la diffusion de documents scientifiques de niveau recherche, publiés ou non, émanant des établissements d'enseignement et de recherche français ou étrangers, des laboratoires publics ou privés.

Tracking of Coordinated Groups using Marginalised MCMC-Based Particle Algorithm

François Septier, Sze Kim Pang, Simon Godsill and Avishy Carmi
Signal Processing Laboratory
Cambridge University Engineering Department, UK
{fjms2,skp31,sjg30,ac599}@cam.ac.uk

Abstract

In this paper, we address the problem of detection and tracking of group and individual targets. In particular, we focus on a group model with a virtual leader which models the bulk or group parameter. To perform the sequential inference, we propose a Markov Chain Monte Carlo (MCMC)-based Particle algorithm with a marginalisation scheme using pairwise Kalman filters. Numerical simulations illustrate the ability of the algorithm to detect and track targets within groups, as well as infer both the correct group structure and the number of targets over time.

TABLE OF CONTENTS

1 INTRODUCTION	1
2 GROUP DYNAMICAL MODEL	2
3 BAYESIAN MODELING	4
4 BAYESIAN SOLUTION	8
5 NUMERICAL RESULTS	12
6 CONCLUSIONS	13
ACKNOWLEDGEMENTS	14
REFERENCES	14
BIOGRAPHY	16

1. INTRODUCTION

The purpose of multiple target tracking algorithms is to detect, track and identify targets from sequences of noisy observations of the targets provided by one or more sensors. The difficulty of this problem has increased as sensor systems in the modern battlefield are required to detect and track targets in very low probability of detection and in hostile environments with heavy clutter. A common assumption in the target tracking literature is that each target moves independently of all others. However, in practice, this is not always true as targets may move in a common formation; for example, a group of aircraft moving in a tight formation or a convoy of vehicles moving along a road. If the dependencies of the group objects can be exploited, it can potentially lead to better detection and tracking performances, especially in hostile environments with high noise and low detection probabilities.

In [1], the authors investigated a method for group object tracking by using a dynamical model with a ‘bulk’ component that describes the evolution of the group. However, the paper assumes that the group structure is known with a fixed number of targets. In [2], a spatial distribution model for tracking extended objects in clutter was introduced. Based on this approach, a Poisson likelihood model for extended and group object were developed in [3, 4]. In [5, 6], Mahler derived methods for tracking group-targets based on random-sets techniques, *i.e.* the ‘bulk’ of targets but not the individual targets. In [7], Clark and Godsill proposed a Gaussian mixture Probability Hypothesis Density filter (PHD) to identify group targets and their constituent members by creating a graph of connected components. More recently in [8], the authors presented a survey of work done on group tracking and proposed two novel group dynamical models, a basic model and a group model with a virtual leader. They are formulated within a continuous time setting and include a repulsive force mechanism for modeling interactions between closely spaced targets. A Markov Chain Monte Carlo (MCMC) Particles algorithm is then proposed to approximate the filtering posterior distribution for the group tracking problem using the basic model.

In this paper, we focus on the group model with a virtual leader. As opposed to the basic model which used a deterministic function of the targets to characterise the bulk group motion, this model has more flexible behaviour owing to the independence of the virtual leader from the targets. To solve the problem of the group structure inference and joint detection and tracking for group and individual targets, we propose a MCMC-based Particle algorithm with some improvements in the choice of the proposal distribution compared to the one in [8]. Moreover, the linear and Gaussian sub-structure contained in the group dynamical model is exploited through a marginalisation scheme using pairwise Kalman filters for the propagation of the sufficient

statistics. The proposed marginalised method allows a dramatic reduction in the state-space dimension by a factor of 2.5, thus improving the variance of the final estimates.

The paper is organised as follows. In Section 2, the group dynamical model with a virtual leader is described in a continuous time setting. Section 3 develops the group tracking model in a Bayesian framework. The proposed inference algorithm is detailed in Section 4. Numerical results are shown in Section 5. Conclusions are given in Section 6.

2. GROUP DYNAMICAL MODEL

Group Model with Virtual Leader

The idea of group modeling is to adopt a behavioural model in which each member of a group interacts with the other members of the group, typically making its velocity and position more similar to that of others in the same group. In [8], this idea has been conveniently formulated in continuous time through a multivariate stochastic differential equation (SDE) and then derived in discrete time without approximation error, owing to the assumed linear and Gaussian form for the model. In particular, two different models have been proposed. In the first, the basic group model, the group parameter is modeled as a deterministic function of the targets. In the second, the group model with a virtual leader, an additional state variable is introduced in order to model the bulk or group parameter. This second approach is closer in spirit to the bulk velocity model [9] and virtual leader-follower model [10]. This model provides a more flexible behaviour since the virtual leader is no longer a deterministic function of the individual target states. In this paper, we focus our study on this virtual leader model in which the spatio-temporal structure for the i^{th} target in a group, g , has been defined in [8] by :

$$d\hat{x}_{t,i}^g = \left\{ -\alpha[x_{t,i}^g - v_t^{g,x}] - \gamma_1 \hat{x}_{t,i}^g - \beta[\hat{x}_{t,i}^g - \hat{v}_t^{g,x}] \right\} dt + \sigma_x dW_{t,i}^{g,x} \quad (1)$$

$$d\hat{v}_t^{g,x} = -\gamma_2 \hat{v}_t^{g,x} dt + \sigma_g dG_t^{g,x} \quad (2)$$

Here $x_{t,i}^g$ is the Cartesian position in the X direction of the i^{th} target in the group g at time t , with $\hat{x}_{t,i}^g$ the corresponding velocity. $v_t^{g,x}$ and $\hat{v}_t^{g,x}$ represent respectively the Cartesian position and the velocity both in the X direction of the unobserved virtual leader of the group g . $W_{t,i}^{g,x}$ and $G_t^{g,x}$ are two independent standard Brownian motion. $W_{t,i}^{g,x}$ is assumed to be independtly generated for each target i in the group. The parameters α , β and γ_1 are positive, and reflect the strength of the pull towards the group bulk. The ‘mean reversion’ terms $\gamma_1 \hat{x}_{t,i}^g$ and $\gamma_2 \hat{v}_t^{g,x}$ simply prevent the velocities of the target and the virtual leader respectively drifting up to very large values with time.

The joint state corresponding to N_g targets in the g^{th} group can thus be written in a matrix form as follows :

$$ds_t^g = \mathbf{A}^g \mathbf{s}_t^g dt + \mathbf{D}^g d\mathbf{n}_t^g \quad (3)$$

where the state is defined as $\mathbf{s}_t^g = [(\mathbf{x}_t^g)^T (\mathbf{v}_t^g)^T]^T$, $\mathbf{x}_t^g = [x_{t,1}^g \dots x_{t,N_g}^g \ y_{t,1}^g \dots y_{t,N_g}^g \ \hat{x}_{t,1}^g \dots \hat{x}_{t,N_g}^g \ \hat{y}_{t,1}^g \dots \hat{y}_{t,N_g}^g]^T$, $\mathbf{v}_t^g = [v_t^{g,x} \ v_t^{g,y} \ \hat{v}_t^{g,x} \ \hat{v}_t^{g,y}]^T$ and the transition matrix $\mathbf{A}^g \in \mathbb{R}^{4(N_g+1) \times 4(N_g+1)}$ is defined as

$$\mathbf{A}^g = \begin{bmatrix} \mathbf{0}_{2N_g \times 2N_g} & \mathbf{I}_{2N_g} & \mathbf{0}_{2N_g \times 4} \\ -\alpha \mathbf{I}_{2N_g} & (-\beta - \gamma_1) \mathbf{I}_{2N_g} & \Lambda_a^g \\ \mathbf{0}_{4 \times 2N_g} & \mathbf{0}_{4 \times 2N_g} & \Lambda_b^g \end{bmatrix} \quad (4)$$

with

$$\Lambda_a^g = \begin{bmatrix} \alpha \mathbf{1}_{N_g \times 1} & \mathbf{0}_{N_g \times 1} & \beta \mathbf{1}_{N_g \times 1} & \mathbf{0}_{N_g \times 1} \\ \mathbf{0}_{N_g \times 1} & \alpha \mathbf{1}_{N_g \times 1} & \mathbf{0}_{N_g \times 1} & \beta \mathbf{1}_{N_g \times 1} \end{bmatrix} \quad (5)$$

and,

$$\Lambda_b^g = \begin{bmatrix} 0 & 0 & 1 & 0 \\ 0 & 0 & 0 & 1 \\ 0 & 0 & -\gamma_2 & 0 \\ 0 & 0 & 0 & -\gamma_2 \end{bmatrix} \quad (6)$$

The matrix $\mathbf{D}^g \in \mathbb{R}^{4(N_g+1) \times 2(N_g+1)}$ is defined as

$$\mathbf{D}^g = \begin{bmatrix} \mathbf{0}_{2N_g \times 2N_g} & \mathbf{0}_{2N_g \times 2} \\ \mathbf{I}_{2N_g} & \mathbf{0}_{2N_g \times 2} \\ \mathbf{0}_{2 \times 2N_g} & \mathbf{0}_{2 \times 2} \\ \mathbf{0}_{2 \times 2N_g} & \mathbf{I}_2 \end{bmatrix} \quad (7)$$

dn_t^g is a Brownian motion with covariance matrix $\mathbf{Q}_c^g = \text{diag}[\sigma_x^2, \dots, \sigma_x^2, \sigma_y^2, \dots, \sigma_y^2, \sigma_g^2, \sigma_g^2]$.

Repulsive Force

The above model can model interacting behaviour of targets which belong to a same group. However in order to reduce or eliminate behaviour in which targets become collocated or collide spatially, which are clearly infeasible or highly unlikely in practice, some modifications to the model must be introduced. In [11, 12], an interaction model is specified in terms of a Markov Random Field. This approach can model rather complicated behaviour but it can present some challenges in inference as the normalisation constants are in general unknown in closed form for these models.

In [8], the authors proposed another method using a switching mode model that can deliver repulsive forces when targets become too close spatially. In this paper, we will consider this approach since it is simpler computationally as compared to the MRF model. By using the same approach as in [8], the original SDE in Eq. (3) can be written as :

$$ds_t^g = \mathbf{A}^g s_t^g dt + \mathbf{h}^g dt + \mathbf{D}^g dn_t^g \quad (8)$$

where $\mathbf{h}^g = [\mathbf{0}_{1 \times 4} \hat{r}_{1,2}^x - \hat{r}_{1,2}^x \hat{r}_{1,2}^y - \hat{r}_{1,2}^y \mathbf{0}_{1 \times 4}]^T$ models the repulsive forces as a fixed constant value between time t and $t + \tau$ for a group of two targets. $\hat{r}_{1,2}$ is calculated using the state configuration at time t as follows :

$$\begin{bmatrix} \hat{r}_{1,2}^x \\ \hat{r}_{1,2}^y \end{bmatrix} = \frac{f_{t,1,2}}{d_{t,1,2}} \left(\begin{bmatrix} x_{t,1} \\ y_{t,1} \end{bmatrix} - \begin{bmatrix} x_{t,2} \\ y_{t,2} \end{bmatrix} \right) \quad (9)$$

$$d_{t,1,2} = \{(x_{t,1} - x_{t,2})^2 + (y_{t,1} - y_{t,2})^2\}^{\frac{1}{2}} \quad (10)$$

$$f_{t,1,2} = \frac{R_1}{d_{t,1,2} + R_2} \quad (11)$$

The SDE (8) has a simple solution :

$$\mathbf{s}_{t+\tau}^g = e^{\mathbf{A}^g \tau} \mathbf{s}_t^g + \int_{l=t}^{l=t+\tau} e^{\mathbf{A}^g (t+\tau-l)} (\mathbf{h}^g dl + \mathbf{D}^g dn_l^g) \quad (12)$$

The distribution of \mathbf{s}_t^g is thus given by a Normal distribution :

$$p_u(\mathbf{s}_t^g | \mathbf{s}_{t-1}^g) = \mathcal{N}(\mathbf{s}_t^g | \mathbf{F}_{N_g} \mathbf{s}_{t-1}^g + \mathbf{R}_{N_g} \mathbf{h}^g, \mathbf{Q}_{N_g}) \quad (13)$$

with

$$\mathbf{F}_{N_g} = e^{\mathbf{A}^g \tau} \quad (14)$$

$$\mathbf{R}_{N_g} = \int_{l=t}^{l=t+\tau} e^{\mathbf{A}^g (t+\tau-l)} dl \quad (15)$$

$$\mathbf{Q}_{N_g} = \int_{l=t}^{l=t+\tau} e^{\mathbf{A}^g (t+\tau-l)} \mathbf{D}^g \mathbf{Q}_c^g (\mathbf{D}^g)^T e^{\mathbf{A}^g (t+\tau-l)^T} dl \quad (16)$$

If integrals involved in Eqs. (15) and (16) cannot be computed directly, the matrices \mathbf{R}_{N_g} and \mathbf{Q}_{N_g} can be efficiently obtained by the matrix fraction decomposition [13, 14] as described in [8].

As an illustration, Figure 1 shows a realisation of the dynamical model Eq. (13) for 4 targets. The scenario consists of 4 targets moving together as a group. The parameters used to generate the tracks can be found in Table 1. The resulting tracks generally correspond to moving ground vehicles.

3. BAYESIAN MODELING

After having described the group dynamical model, we can now formulate the group tracking problem in a Bayesian framework by introducing the target birth and death process, the group structure transition model and the observation model. This section follows quite closely the methodology of [8].

First, the target states are variable dimension quantities since targets can appear or disappear from the scene randomly over time. In order to model this birth and death process, we choose to use a set of existence variables \mathbf{e}_t with elements $e_{t,i} \in \{0, 1\}$

Simulation Parameters	Symbol	Value
Time interval between samples	τ	5 seconds
Actual number of targets	N	4
Number of simulation time steps		110
Centroid control parameter	α	0.0006
Group velocity control parameter	β	0.05
Velocity control parameter	$\gamma_1 = \gamma_2$	0.001
Individual motion noise	σ_x	0.2
Group motion noise	σ_g	0.5
Repulsive force constants	R_1	8
	R_2	12

Table 1. Track Simulation Parameters for Moving Ground Vehicles

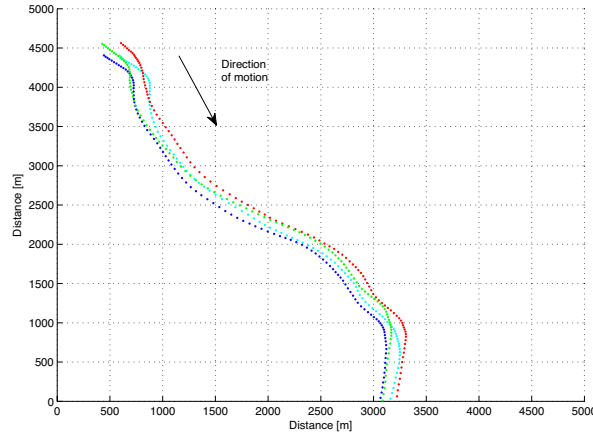


Figure 1. Motion of 4 targets in a group using the virtual leader model and the repulsive forces.

model the birth and death process for each individual target. In this formulation, the targets' kinematic vector is thus regarded as fixed dimensional quantity with N_{max} targets, each of which being active or inactive according to its existence variable $e_{t,i}$.

We use \mathbf{g}_t to represent the group structure at the time t . For example, for 5 targets, the group structure representation $\mathbf{g}_t = [1 \ 1 \ 2 \ 3 \ 3]^T$ means, as illustrated in Figure 2, that targets $\{1,2\}$ are in group 1, target $\{3\}$ is in group 2 and targets $\{4,5\}$ are in group 3. With the use of the dynamical model described in the previous section, each group has also its own virtual leader. As a consequence, the state \mathbf{s}_t has a dimension of $(8N_{max} \times 1)$ since the maximum number of groups is N_{max} which corresponds to the case where each target belongs to a different group (*i.e.* $\mathbf{g}_t = [1 \ 2 \ 3 \ 4 \ 5]^T$ for $N_{max} = 5$). The state \mathbf{s}_t to infer is thus composed of $\mathbf{x}_t = [x_{t,1}, \dots, x_{t,N_{max}}, y_{t,1}, \dots, y_{t,N_{max}}, \dot{x}_{t,1}, \dots, \dot{x}_{t,N_{max}}, \dot{y}_{t,1}, \dots, \dot{y}_{t,N_{max}}]$ and $\mathbf{v}_t = [v_t^{1,x}, \dots, v_t^{N_{max},x}, v_t^{1,y}, \dots, v_t^{N_{max},y}]^T$.

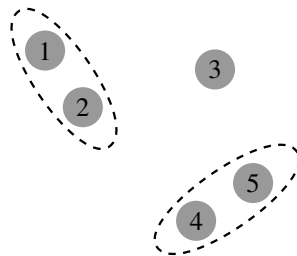


Figure 2. Illustration of the group structure $\mathbf{g}_t = [1 \ 1 \ 2 \ 3 \ 3]^T$.

In a Bayesian context, the aim is to compute the posterior distribution $p(\mathbf{s}_{0:t}, \mathbf{g}_{0:t}, \mathbf{e}_{0:t} | \mathbf{Z}_{1:t})$ where $\mathbf{Z}_{1:t}$ corresponds to the observation set from time 1 to t . By using the Bayes' theorem, this distribution is given recursively by :

$$\begin{aligned} p(\mathbf{s}_{0:t}, \mathbf{g}_{0:t}, \mathbf{e}_{0:t} | \mathbf{Z}_{1:t}) &= \frac{p(\mathbf{s}_{0:t-1}, \mathbf{g}_{0:t-1}, \mathbf{e}_{0:t-1} | \mathbf{Z}_{1:t-1})}{p(\mathbf{Z}_t | \mathbf{Z}_{1:t-1})} \\ &\times p(\mathbf{s}_t, \mathbf{g}_t, \mathbf{e}_t | \mathbf{s}_{0:t-1}, \mathbf{g}_{0:t-1}, \mathbf{e}_{0:t-1}) \\ &\times p(\mathbf{Z}_t | \mathbf{s}_t, \mathbf{g}_t, \mathbf{e}_t) \end{aligned} \quad (17)$$

Moreover, we propose to expand the transition probability distribution as follows :

$$\begin{aligned} &p(\mathbf{s}_t, \mathbf{g}_t, \mathbf{e}_t | \mathbf{s}_{0:t-1}, \mathbf{g}_{0:t-1}, \mathbf{e}_{0:t-1}) \\ &= p(\mathbf{s}_t, \mathbf{e}_t | \mathbf{s}_{0:t-1}, \mathbf{e}_{0:t-1}, \mathbf{g}_{0:t}) p(\mathbf{g}_t | \mathbf{s}_{0:t-1}, \mathbf{g}_{0:t-1}, \mathbf{e}_{0:t-1}) \end{aligned} \quad (18)$$

where $p(\mathbf{g}_t | \mathbf{s}_{0:t-1}, \mathbf{g}_{0:t-1}, \mathbf{e}_{0:t-1})$ is the discrete probability distribution of the group structure transition and $p(\mathbf{s}_t, \mathbf{e}_t | \mathbf{s}_{0:t-1}, \mathbf{e}_{0:t-1}, \mathbf{g}_{0:t})$ is the prior distribution of the targets, the virtual leaders and the existence variables given their past values and the group structure upon to time t . We now described the various models.

Group structure transition model

The modeling of the group structure evolution clearly depends on the type of group targets we are dealing with. However, generally, we expect to observe only small changes in group structure over short time intervals. Moreover, certain group structure would be considered highly unlikely. For example, two targets that are widely separated are unlikely to join together within one group. In this paper, we adopt the following model for the group transition probability :

$$\begin{aligned} p(\mathbf{g}_t | \mathbf{s}_{0:t-1}, \mathbf{g}_{0:t-1}, \mathbf{e}_{0:t-1}) &= P_{NC} \delta(\mathbf{g}_t - \mathbf{g}_{t-1}) \\ &+ (1 - P_{NC}) \pi(\mathbf{g}_t | \mathbf{s}_{0:t-1}, \mathbf{g}_{0:t-1}, \mathbf{e}_{0:t-1}) \end{aligned} \quad (19)$$

where $\delta(\cdot)$ is the Dirac delta function. $P_{NC} \in [0, 1]$ is used to ensure that only small changes in group structure over short time intervals occur and $\pi(\mathbf{g}_t | \mathbf{s}_{0:t-1}, \mathbf{g}_{0:t-1}, \mathbf{e}_{0:t-1})$ denotes the discrete probability of the group structure transition at time t which is an important term in this model. In this paper, we have adopted a state dependent model in which the current group structure depends only on both the target positions, denoted by $\mathbf{x}_{p,t}$, and the existence variables at time $t - 1$, *i.e.*

$$\pi(\mathbf{g}_t | \mathbf{s}_{0:t-1}, \mathbf{g}_{0:t-1}, \mathbf{e}_{0:t-1}) = \pi(\mathbf{g}_t | \mathbf{x}_{p,t-1}, \mathbf{e}_{t-1}) \quad (20)$$

This distribution determines how information from \mathbf{x}_{t-1} and \mathbf{e}_{t-1} can be used to guide group changes. For a pair of targets i and j , suppose we can define a quantity $q_{i,j}$ which gives an indication of how likely they are to be in a same group at time t . For each group structure \mathbf{h} , let Δ be the set of all pairs of targets that belong to the same group. We can then calculate the following scoring function :

$$f(\mathbf{g}_t = \mathbf{h} | \mathbf{x}_{p,t-1}, \mathbf{e}_{t-1}) = \prod_{i,j \in \Delta} q_{i,j} \prod_{i,j \notin \Delta} (1 - q_{i,j}) \quad (21)$$

As a consequence, we define the density $\pi(\mathbf{g}_t | \mathbf{x}_{p,t-1}, \mathbf{e}_{t-1})$ as :

$$\pi(\mathbf{g}_t | \mathbf{x}_{p,t-1}, \mathbf{e}_{t-1}) = \frac{f(\mathbf{g}_t = \mathbf{h} | \mathbf{x}_{p,t-1}, \mathbf{e}_{t-1})}{\sum_{\forall \mathbf{h}'} f(\mathbf{g}_t = \mathbf{h}' | \mathbf{x}_{p,t-1}, \mathbf{e}_{t-1})} \quad (22)$$

Now, the function $q_{i,j}$ involved in the computation of the scoring function, is defined as :

$$q_{i,j} = \begin{cases} P_Q & \text{if } e_{t,i} = 0 \text{ or } e_{t,j} = 0 \\ h(\mathbf{x}_{p,t-1,i}, \mathbf{x}_{p,t-1,j}) & \text{otherwise} \end{cases} \quad (23)$$

$h(\mathbf{x}_{p,t-1,i}, \mathbf{x}_{p,t-1,j})$ can be any function that assigns values between 0 and 1 depending on how close a pair of targets must be before they are considered likely to be in a group. P_Q is a small positive value allowing for inactive target to be grouped with active targets.

The joint prior distribution of the targets and their existence variables

Each target's existence variable will be modeled as a discrete Markov chain [15] which is independent of all other states :

$$\begin{aligned} p(\mathbf{s}_t, \mathbf{e}_t | \mathbf{s}_{0:t-1}, \mathbf{e}_{0:t-1}, \mathbf{g}_{0:t}) &= p(\mathbf{s}_t | \mathbf{s}_{0:t-1}, \mathbf{e}_{0:t}, \mathbf{g}_{0:t}) \\ &\times \prod_{i=1}^{N_{max}} p(e_{t,i} | e_{t-1,i}) \end{aligned} \quad (24)$$

In this paper, the transition probability for the existence variable is defined as follows :

$$\begin{aligned}
p(e_{t,i}|e_{t-1,i}) &= \delta(e_{t,i} - 1) [(1 - P_D)\delta(e_{t-1,i} - 1) \\
&\quad + P_B\delta(e_{t-1,i})] + \delta(e_{t,i}) [(1 - P_B)\delta(e_{t-1,i}) \\
&\quad + P_D\delta(e_{t-1,i} - 1)]
\end{aligned} \tag{25}$$

where P_B and P_D are probability values for a target to become respectively active ('alive') or inactive ('dead').

Now, let us identify the transition probability for \mathbf{s}_t . We can firstly partition targets according to \mathbf{e}_t and \mathbf{e}_{t-1} using Eq. (24). Let $\Upsilon = \{1, 2, \dots, N_{max}\}$ and $\Upsilon(h, \mathbf{g}_t)$ be the set of targets that belong to group h of group structure \mathbf{g}_t . Let us introduce now the following different sets :

$$\begin{aligned}
\Upsilon_1 &= \{i \in \Upsilon | e_{t,i} = 0\} \\
\Upsilon_2 &= \{i \in \Upsilon | (e_{t,i} = 1) \wedge (e_{t-1,i} = 0)\} \\
\Upsilon_3 &= \{i \in \Upsilon | (e_{t,i} = 1) \wedge (e_{t-1,i} = 1)\} \\
\Upsilon_4 &= \{i \in \Upsilon | \forall k \in \Upsilon(i, \mathbf{g}_t) : e_{t,k} = 0\} \\
\Upsilon_5 &= \{i \in \Upsilon | \exists k \in \Upsilon(i, \mathbf{g}_t) : (e_{t,k} = 1) \wedge (e_{t-1,k} = 1)\} \\
\Upsilon_6 &= \Upsilon \setminus (\Upsilon_4 \cup \Upsilon_5)
\end{aligned} \tag{26}$$

Υ_1 corresponds to the set of inactive targets. Υ_2 is the set of targets which become active, thus representing the birth scenario. Υ_3 is the set of active targets that will be updated according the continuous time group model described in Section 2. Υ_4 corresponds to the set of groups in which all targets are inactive. Υ_5 is the set of groups in which at least one target remains alive. Finally, Υ_6 represents the set of new groups. This case occurs typically when at least one target in a group become alive and the other ones are inactive. Once these different sets are introduced, the joint transition probability for \mathbf{x}_t and \mathbf{v}_t can be written as :

$$\begin{aligned}
p(\mathbf{s}_t | \mathbf{s}_{0:t-1}, \mathbf{e}_{0:t}, \mathbf{g}_{0:t}) &= p(\mathbf{x}_t, \mathbf{v}_t | \mathbf{x}_{0:t-1}, \mathbf{v}_{0:t-1}, \mathbf{e}_{0:t}, \mathbf{g}_{0:t}) \\
&= p_u(\mathbf{x}_t, \Upsilon_3, \mathbf{v}_t, \Upsilon_5 | \mathbf{x}_{0:t-1}, \mathbf{v}_{0:t-1}, \mathbf{e}_{0:t}, \mathbf{g}_{0:t}) \\
&\quad \times \prod_{i \in \Upsilon_1} p_{d_T}(\mathbf{x}_{t,i}) \prod_{j \in \Upsilon_2} p_{b_T}(\mathbf{x}_{t,j} | \mathbf{x}_{0:t-1}, \mathbf{e}_{0:t}, \mathbf{g}_{0:t}) \\
&\quad \times \prod_{k \in \Upsilon_4} p_{d_{V_L}}(\mathbf{v}_{t,k}) \prod_{l \in \Upsilon_6} p_{b_{V_L}}(\mathbf{v}_{t,l} | \mathbf{x}_{0:t}, \mathbf{e}_{0:t}, \mathbf{g}_{0:t})
\end{aligned} \tag{27}$$

Birth scenario—A target birth happens when $e_{t,i} = 1$ and $e_{t-1,i} = 0$. However, as it is possible for an inactive target to be grouped with other active targets, this leads to the possibility of having a target birth with its initial kinematics being some function of the average group behaviour. Consequently, let partition the set Υ_2 into two subsets as follows :

$$\begin{aligned}
\Upsilon_2^1 &= \{i \in \Upsilon_2 | g_{t,i} \in (\Upsilon_4 \cup \Upsilon_6)\} \\
\Upsilon_2^2 &= \{i \in \Upsilon_2 | g_{t,i} \in \Upsilon_5\}
\end{aligned} \tag{28}$$

where Υ_2^2 is the set of target belonging to a group in which at least one target is active. This case corresponds to the group target birth. Υ_2^1 is the set of targets becoming alive and belonging to a group without active target at both the previous and current time. In this second case, the targets will be initialised independently using some initial distribution.

For a group target birth, we can calculate the average group state at time $t - 1$ and move according to the single target dynamic. As a consequence, if $j \in \Upsilon_2^2$ and this target belongs to the h^{th} group, we have:

$$\mathbf{x}_{t,j} \sim \mathcal{N}(\tilde{\mathbf{F}}_1 \bar{\mathbf{s}}_{t-1}, \mathbf{Q}_{b_T}) \tag{29}$$

with $\bar{\mathbf{s}}_{t-1} = [\bar{\mathbf{x}}_{t-1}^T \mathbf{v}_{t-1}^T]^T$,

$$\bar{\mathbf{x}}_{t-1} = \frac{1}{N_{\Upsilon_3^h}} \sum_{i \in \Upsilon_3^h} \mathbf{x}_{t-1,i} \tag{30}$$

and

$$\tilde{\mathbf{F}}_1 = [\mathbf{I}_4 \quad \mathbf{0}_{4 \times 4}] \mathbf{F}_1 \tag{31}$$

with $\Upsilon_3^h = \{i \in (\Upsilon_3 \cap \Upsilon(h, \mathbf{g}_t))\}$ the set of targets remaining alive and belonging to the same group h , $N_{\Upsilon_3^h}$ the number of targets in this set and \mathbf{F}_1 defined in Eq. (14).

For target birth, if $j \in \Upsilon_2^1$, $\mathbf{x}_{t,j}$ is initialised using an initial probability distribution $p_0(\mathbf{x}_{t,j})$. Since a target can appear anywhere uniformly in the surveillance area of L_x by L_y , a uniform distribution is chosen for the target's initial position. The initial velocity is chosen to be distributed as a zero mean Gaussian variable with variance $\sigma_{V_{max}}^2$:

$$\begin{aligned} x_{t,j} &\sim \mathcal{U}(x_{t,j}|0, L_x) \\ y_{t,j} &\sim \mathcal{U}(y_{t,j}|0, L_y) \\ \dot{x}_{t,j} &\sim \mathcal{N}(\dot{x}_{t,j}|0, \sigma_{V_{max}}^2) \\ \dot{y}_{t,j} &\sim \mathcal{N}(\dot{y}_{t,j}|0, \sigma_{V_{max}}^2) \end{aligned} \quad (32)$$

and thus

$$\begin{aligned} p_0(\mathbf{x}_{t,j}) &= \mathcal{U}(x_{t,j}|0, L_x)\mathcal{U}(y_{t,j}|0, L_y) \\ &\times \mathcal{N}(\dot{x}_{t,j}|0, \sigma_{V_{max}}^2)\mathcal{N}(\dot{y}_{t,j}|0, \sigma_{V_{max}}^2) \end{aligned} \quad (33)$$

Hence, the birth probability, including both the group target birth and the target birth, is given by :

$$p_{b_T}(\mathbf{x}_{t,j}|\mathbf{x}_{0:t-1}, \mathbf{e}_{0:t}, \mathbf{g}_{0:t}) = \begin{cases} p_0(\mathbf{x}_{t,j}) & \text{if } j \in \Upsilon_2^1 \\ \mathcal{N}(\mathbf{F}_1 \bar{\mathbf{s}}_{t-1}, \mathbf{Q}_{b_T}) & \text{if } j \in \Upsilon_2^2 \end{cases} \quad (34)$$

The virtual leader corresponding to the h^{th} group have to be initialised if $h \in \Upsilon_6$. This case happens when at least one target belonging to this h^{th} group becomes active using $p_0(\mathbf{x}_{t,j})$. In this case, the proposed virtual leader initial probability is given by :

$$\begin{aligned} p_{b_{VL}}(\mathbf{v}_{t,h}|\mathbf{x}_{0:t}, \mathbf{e}_{0:t}, \mathbf{g}_{0:t}) &= \mathcal{N}\left(\frac{1}{N_{\Upsilon_2 \cap \Upsilon(h, \mathbf{g}_t)}} \right. \\ &\left. \times \sum_{i \in \Upsilon_2 \cap \Upsilon(h, \mathbf{g}_t)} \mathbf{x}_{t,i}, \mathbf{Q}_{b_{VL}}\right) \end{aligned} \quad (35)$$

Death scenario—For inactive targets, *i.e.* $i \in \Upsilon_1$, we will keep the target state at some \mathbf{x}_{death} corresponding to the state where inactive target is represented :

$$p_{d_T}(\mathbf{x}_{t,i}) = \delta(\mathbf{x}_{death}) \quad (36)$$

In a similar way, \mathbf{v}_{death} is used to characterise a virtual leader of a group in which all targets are inactive, *i.e.* for $h \in \Upsilon_4$:

$$p_{d_{VL}}(\mathbf{v}_t^h) = \delta(\mathbf{v}_{death}) \quad (37)$$

Update scenario—The targets, which remain active between two time samples, and their associated virtual leader are updated according to the dynamical model in Eq. (13). However, the merging and splitting of groups of targets has to be considered. On the one hand, for a merging scenario at time t , Eq. (13) becomes :

$$p_u(\mathbf{s}_t^g|\mathbf{s}_{t-1}) = \mathcal{N}(\mathbf{s}_t^g|\mathbf{F}_{N_g}[\mathbf{x}_t^g, \bar{\mathbf{v}}_t] + \mathbf{R}_{N_g} \mathbf{h}^g, \mathbf{Q}_{N_g}) \quad (38)$$

where $\bar{\mathbf{v}}_t$ is the average of the virtual leader kinematics of the merging groups.

On the other hand, in the case of splitting, the different \mathbf{s}_t^g from the splitting are updated with Eq. (13) by using the same virtual leader at the previous time sample $t - 1$.

Observation model

To complete the Bayesian model, we will need to specify an observation model. Nonlinear filtering techniques such as particle filter and MCMC provides much more flexibility to model the sensor measurements. As a result, the association free approach can be taken [9, 16].

There are several important advantages to this approach. Firstly, more complicated sensor models can be used, such as those involving merged multiple target measurements, and radar range and velocity ambiguity. For example, in an image sensor, depending on the nature of the optics and their impulse response function after processing, a target often contribute to two or more pixels. Similarly, two or more targets can contributed to the output of a single pixel. Related to this, the approach also enable the use of unthresholded measurements which will enable improved tracking at lower target SNR [17, 18]. This is

popularly known as Track-Before-Detect (TBD). Secondly, it avoids the combinatorial problem of explicit enumeration of the track and data association.

In this framework, it is assumed that at each time step t , a pixel grid of $N_{pix}^x \times N_{pix}^y$ resolution cells is read simultaneously and each individual pixel (i, j) has an intensity of z_t^{ij} . In general, z_t^{ij} can be thresholded ($z_t^{ij} = 1$ or 0) or non-thresholded. By considering $\mathbf{Z}_t = \left\{ z_t^{ij} \right\}_{i=1, j=1}^{N_{pix}^x, N_{pix}^y}$ to be a set of observations obtained from a sensor scan, the pixel measurements are modeled as conditionally independent given the states $\mathbf{x}_{p,t}$ and \mathbf{e}_t ,

$$p(\mathbf{Z}_t | \mathbf{x}_{p,t}, \mathbf{e}_t) = \prod_{i,j} p(z_t^{ij} | \mathbf{x}_{p,t}, \mathbf{e}_t) \quad (39)$$

Each pixel can couple to multiple targets and a single target can affect the output of multiple pixels. Let $\kappa_{t,n}$ be the sub-set of pixel measurements in \mathbf{Z}_t such that they are coupled with the n^{th} target. If the n^{th} target is inactive, *i.e.* $e_{t,n} = 0$, then $\kappa_{t,n}$ is an empty set. κ_t will be defined as the union of all the sets of $\kappa_{t,n}$, *i.e.* $\kappa_t = \kappa_{t,1} \cup \kappa_{t,2} \cup \dots \cup \kappa_{t,N_{max}}$. Also let $\kappa_{t,0}$ be the subset of pixel measurements that are not coupled to any target and they are characterized solely by the background clutter model $p_C(z_t^{ij})$. Then,

$$\begin{aligned} p(\mathbf{Z}_t | \mathbf{x}_{p,t}, \mathbf{e}_t) &= \prod_{i,j \in \kappa_t} p(z_t^{ij} | \mathbf{x}_{p,t}) \prod_{i,j \in \kappa_{t,0}} p_C(z_t^{ij}) \\ &\propto \prod_{i,j \in \kappa_t} \frac{p(z_t^{ij} | \mathbf{x}_{p,t}, \mathbf{e}_t)}{p_C(z_t^{ij})} \end{aligned} \quad (40)$$

For the synthetic data simulation, we will specify the observation model as a simplified ground moving target indicator (GMTI) radar with position only Rayleigh-distributed measurements [16]. We will also use thresholded measurement that returns 1 or 0 for each pixel. Then, the probability of detection $P_{d,n}$ for n targets in a pixel given that the background false alarm probability, P_{fa} , is

$$P_{d,n} = P_{fa}^{\frac{1}{1+n \times SNR}} \quad (41)$$

4. BAYESIAN SOLUTION

The filtering distribution of interest is complex and highly nonlinear. Sequential Monte Carlo methods such as particle filters can be used to carry out the inference. However, given the high dimensionality of the state space, it will not be straightforward to design an efficient particle filter implementation. In this section, we introduce the new marginalised approach to the virtual leader model.

Traditionally, MCMC is used to draw samples from probability distributions in a non-sequential setting. The advantages of MCMC are that it is generally more effective than particle filters in high-dimensional systems and it is easier to design for complex distributions if it can be used in a sequential fashion. Sequential approaches using MCMC can be found in [8, 11, 19, 20]. In [19], a sequential MCMC algorithm was designed to do inference in dynamical models using a series of Metropolis-Hastings-within-Gibbs. A similar idea was applied in [20] for imputing missing data from nonlinear diffusion. In [11], a MCMC-Particles algorithm was proposed using a numerical integration of the predictive density but unfortunately its computational demand can become excessive as the number of particles increases owing to its direct Monte Carlo calculation of the filtering density at each time step. In this paper, we will design an improved version of the MCMC-Particles algorithm proposed in [8] to do the sequential inference. The approach is also distinct from the Resample-Move scheme [21] in particle filter where the MCMC algorithm is used to rejuvenate degenerate samples following importance sampling resampling: our method uses neither resampling or importance sampling. Moreover, in order to improve the accuracy of the proposed algorithm, both the target velocities and the virtual leader kinematics are marginalised.

Marginalisation approach

By using the linear and Gaussian sub-structure of the system, the state space can be reduced significantly by marginalising out the target velocities and the virtual leader kinematics. Indeed, Equation (27) can be written equivalently using the following dynamic state space representation :

$$\begin{bmatrix} \mathbf{x}_{p,t}, \tilde{\Upsilon} \\ \mathbf{x}_{v,t} \\ \mathbf{v}_t \end{bmatrix} = \Psi_t \begin{bmatrix} \mathbf{x}_{p,t-1}, \tilde{\Upsilon} \\ \mathbf{x}_{v,t-1} \\ \mathbf{v}_{t-1} \end{bmatrix} + \mathbf{r}_t + \mathbf{b}_t \quad (42)$$

where $\mathbf{x}_{p,t}$ and $\mathbf{x}_{v,t}$ are the targets' positions and velocities respectively. $\tilde{\Upsilon} = \Upsilon \setminus \Upsilon_2^1$ corresponds to the set of all targets except those that are updated using $p_0(\mathbf{x}_{p,t,j})$ defined in (33). Depending on the current target configuration (*i.e.* $\mathbf{e}_{t-1:t}$, $\mathbf{g}_{t-1:t}$), \mathbf{r}_t is a vector in which elements can correspond to the repulsive forces, \mathbf{x}_{death} , \mathbf{v}_{death} or also null values. Finally, \mathbf{b}_t is a zero-mean Gaussian distributed random vector with a covariance matrix depending also on the current target configuration.

By marginalising out both the target velocities and the virtual leader kinematics, the aim is now to compute the following posterior distribution :

$$\begin{aligned} p(\mathbf{x}_{p,0:t}, \mathbf{g}_{0:t}, \mathbf{e}_{0:t} | \mathbf{Z}_{1:t}) &\propto p(\mathbf{Z}_t | \mathbf{x}_{p,t}, \mathbf{e}_t) p(\mathbf{e}_t | \mathbf{e}_{t-1}) \\ &\quad \times p(\mathbf{g}_t | \mathbf{x}_{p,t-1}, \mathbf{g}_{t-1}, \mathbf{e}_{t-1}) \\ &\quad \times p(\mathbf{x}_{p,t} | \mathbf{x}_{p,0:t-1}, \mathbf{e}_{0:t}, \mathbf{g}_{0:t}) \\ &\quad \times p(\mathbf{x}_{p,0:t-1}, \mathbf{g}_{0:t-1}, \mathbf{e}_{0:t-1} | \mathbf{Z}_{1:t-1}) \end{aligned} \quad (43)$$

The likelihood distribution $p(\mathbf{Z}_t | \mathbf{x}_{p,t}, \mathbf{e}_t)$ and the transition probability for the group $p(\mathbf{g}_t | \mathbf{x}_{p,t-1}, \mathbf{g}_{t-1}, \mathbf{e}_{t-1})$ depend only on the target position $\mathbf{x}_{p,t}$ and are given respectively by (40) and (19). Moreover, the transition probability of the existence variables, defined in (25), is independent of the others states. So, only the prior distribution of the target position is affected by this marginalisation. This distribution can be rewritten as follows :

$$\begin{aligned} p(\mathbf{x}_{p,t} | \mathbf{x}_{p,0:t-1}, \mathbf{e}_{0:t}, \mathbf{g}_{0:t}) &= p_0(\mathbf{x}_{p,t}, \Upsilon_2^1) \\ &\quad \times p(\mathbf{x}_{p,t}, \tilde{\Upsilon} | \mathbf{x}_{p,0:t-1}, \mathbf{e}_{0:t}, \mathbf{g}_{0:t}) \\ &= p_0(\mathbf{x}_{p,t}, \Upsilon_2^1) \\ &\quad \times \int p(\mathbf{w}_{t-1} | \mathbf{x}_{p,0:t-1}, \mathbf{e}_{0:t}, \mathbf{g}_{0:t}) \\ &\quad \times p(\mathbf{x}_{p,t}, \tilde{\Upsilon} | \mathbf{x}_{p,0:t-1}, \mathbf{w}_{t-1}, \mathbf{e}_{0:t}, \mathbf{g}_{0:t}) d\mathbf{w}_{t-1} \end{aligned} \quad (44)$$

with $\mathbf{w}_{t-1} = [\mathbf{x}_{v,t-1}^T \ \mathbf{v}_{t-1}^T]^T$.

In fact, $p(\mathbf{x}_{p,t}, \tilde{\Upsilon} | \mathbf{x}_{p,0:t-1}, \mathbf{e}_{0:t}, \mathbf{g}_{0:t})$ can be viewed as the normalising term involved in the computation of the posterior distribution of the process \mathbf{w}_{t-1} given a set of 'observations' upon to time t $\{\mathbf{x}_{p,0:t-1}, \mathbf{x}_{p,t}, \tilde{\Upsilon}\}$ and $\{\mathbf{e}_{0:t}, \mathbf{g}_{0:t}\}$. Indeed, this distribution is given by

$$\begin{aligned} p(\mathbf{w}_{t-1} | \mathbf{x}_{p,0:t-1}, \mathbf{x}_{p,t}, \tilde{\Upsilon}, \mathbf{e}_{0:t}, \mathbf{g}_{0:t}) &= \\ \frac{p(\mathbf{x}_{p,t}, \tilde{\Upsilon} | \mathbf{x}_{p,0:t-1}, \mathbf{w}_{t-1}, \mathbf{e}_{0:t}, \mathbf{g}_{0:t}) p(\mathbf{w}_{t-1} | \mathbf{x}_{p,0:t-1}, \mathbf{e}_{0:t}, \mathbf{g}_{0:t})}{p(\mathbf{x}_{p,t}, \tilde{\Upsilon} | \mathbf{x}_{p,0:t-1}, \mathbf{e}_{0:t}, \mathbf{g}_{0:t})} \end{aligned} \quad (45)$$

with

$$\begin{aligned} p(\mathbf{w}_{t-1} | \mathbf{x}_{p,0:t-1}, \mathbf{e}_{0:t}, \mathbf{g}_{0:t}) &= \int p(\mathbf{w}_{t-2} | \mathbf{x}_{p,0:t-1}, \mathbf{e}_{0:t}, \mathbf{g}_{0:t}) \\ &\quad \times p(\mathbf{w}_{t-1} | \mathbf{w}_{t-2}, \mathbf{x}_{p,0:t-1}, \mathbf{e}_{0:t}, \mathbf{g}_{0:t}) d\mathbf{w}_{t-2} \end{aligned} \quad (46)$$

and can be considered as the posterior distribution in the following linear and Gaussian model :

$$\begin{bmatrix} \mathbf{x}_{p,t}, \tilde{\Upsilon} \\ \mathbf{w}_t \end{bmatrix} = \begin{bmatrix} \Psi_t^{11} & \Psi_t^{12} \\ \Psi_t^{21} & \Psi_t^{22} \end{bmatrix} \begin{bmatrix} \mathbf{x}_{p,t-1}, \tilde{\Upsilon} \\ \mathbf{w}_{t-1} \end{bmatrix} + \begin{bmatrix} \mathbf{r}_t^1 \\ \mathbf{r}_t^2 \end{bmatrix} + \mathbf{b}_t \quad (47)$$

with

$$\mathbb{E}[\mathbf{b}_t \mathbf{b}_t^T] = \begin{bmatrix} \mathbf{Q}_{b,t}^{11} & \mathbf{Q}_{b,t}^{12} \\ \mathbf{Q}_{b,t}^{21} & \mathbf{Q}_{b,t}^{22} \end{bmatrix} \quad (48)$$

This model in Eq. (47) is a pairwise Markov model [22], which is a generalization of the classical hidden Markov model (HMM) obtained by setting Ψ_t^{12} , Ψ_t^{21} , $\mathbf{Q}_{b,t}^{12}$ and $\mathbf{Q}_{b,t}^{21}$ to matrices of zero. As in the linear and Gaussian HMM, the filtered and predictive posterior distribution, respectively defined as

$$p(\mathbf{w}_{t-1} | \mathbf{x}_{p,0:t-1}, \mathbf{x}_{p,t}, \tilde{\Upsilon}, \mathbf{e}_{0:t}, \mathbf{g}_{0:t}) = \mathcal{N}(\hat{\mathbf{w}}_{t-1|t}, \Sigma_{t-1|t}) \quad (49)$$

$$p(\mathbf{w}_t | \mathbf{x}_{p,0:t-1}, \mathbf{x}_{p,t}, \tilde{\Upsilon}, \mathbf{e}_{0:t}, \mathbf{g}_{0:t}) = \mathcal{N}(\hat{\mathbf{w}}_{t|t}, \Sigma_{t|t}) \quad (50)$$

can be obtained by using the recursive equations of a pairwise Kalman filter [23] :

$$\tilde{\mathbf{x}}_t = \Psi_t^{12} \hat{\mathbf{w}}_{t-1|t-1} + \Psi_t^{11} \mathbf{x}_{p,t}, \tilde{\Upsilon} + \mathbf{r}_t^1 \quad (51)$$

$$\mathbf{L}_t = \mathbf{Q}_{b,t}^{11} + \boldsymbol{\Psi}_t^{12} \boldsymbol{\Sigma}_{t-1|t-1} (\boldsymbol{\Psi}_t^{12})^T \quad (52)$$

$$\mathbf{K}_t = \boldsymbol{\Sigma}_{t-1|t-1} (\boldsymbol{\Psi}_t^{12})^T \mathbf{L}_t^{-1} \quad (53)$$

$$\widehat{\mathbf{w}}_{t-1|t} = \widehat{\mathbf{w}}_{t-1|t-1} + \mathbf{K}_t (\mathbf{x}_{p,t}, \tilde{\boldsymbol{\gamma}} - \tilde{\mathbf{x}}_t) \quad (54)$$

$$\boldsymbol{\Sigma}_{t-1|t} = \boldsymbol{\Sigma}_{t-1|t-1} - \mathbf{K}_t \mathbf{L}_t \mathbf{K}_t^T \quad (55)$$

$$\begin{aligned} \widehat{\mathbf{w}}_{t|t} &= [\boldsymbol{\Psi}_t^{22} - \mathbf{Q}_{b,t}^{21} (\mathbf{Q}_{b,t}^{11})^{-1} \boldsymbol{\Psi}_t^{12}] \widehat{\mathbf{w}}_{t-1|t} \\ &\quad + \mathbf{Q}_{b,t}^{21} (\mathbf{Q}_{b,t}^{11})^{-1} (\mathbf{x}_{p,t}, \tilde{\boldsymbol{\gamma}} - \mathbf{r}_t^1) \\ &\quad + [\boldsymbol{\Psi}_t^{21} - \mathbf{Q}_{b,t}^{21} (\mathbf{Q}_{b,t}^{11})^{-1} \boldsymbol{\Psi}_t^{11}] \mathbf{x}_{p,t-1}, \tilde{\boldsymbol{\gamma}} \\ &\quad + \mathbf{r}_t^2 \end{aligned} \quad (56)$$

$$\begin{aligned} \boldsymbol{\Sigma}_{t|t} &= [\mathbf{Q}_t^{22} - \mathbf{Q}_{b,t}^{21} (\mathbf{Q}_{b,t}^{11})^{-1} \mathbf{Q}_t^{12}] \\ &\quad + [\boldsymbol{\Psi}_t^{22} - \mathbf{Q}_{b,t}^{21} (\mathbf{Q}_{b,t}^{11})^{-1} \boldsymbol{\Psi}_t^{12}] \boldsymbol{\Sigma}_{t-1|t} \\ &\quad \times [\boldsymbol{\Psi}_t^{22} - \mathbf{Q}_{b,t}^{21} (\mathbf{Q}_{b,t}^{11})^{-1} \boldsymbol{\Psi}_t^{12}]^T \end{aligned} \quad (57)$$

The probability $p(\mathbf{x}_{p,t}, \tilde{\boldsymbol{\gamma}} | \mathbf{x}_{p,0:t-1}, \mathbf{e}_{0:t}, \mathbf{g}_{0:t})$ involved in (44) is thus a Gaussian distribution defined by the *innovation* mean vector and covariance matrix of the pairwise Kalman filter :

$$p(\mathbf{x}_{p,t}, \tilde{\boldsymbol{\gamma}} | \mathbf{x}_{p,0:t-1}, \mathbf{e}_{0:t}, \mathbf{g}_{0:t}) = \mathcal{N}(\tilde{\mathbf{x}}_t, \mathbf{L}_t) \quad (58)$$

MCMC-based Particle Algorithm

The aim is to approximate the posterior distribution given by (43). To make the inference from this complex distribution sequentially, we will use a MCMC procedure. Since we do not have the closed form expression of the distribution $p(\mathbf{x}_{p,0:t-1}, \mathbf{g}_{0:t-1}, \mathbf{e}_{0:t-1} | \mathbf{Z}_{1:t-1})$, it will be approximated by an empirical distribution based on the particle set :

$$\begin{aligned} \widehat{p}(\mathbf{x}_{p,0:t-1}, \mathbf{g}_{0:t-1}, \mathbf{e}_{0:t-1} | \mathbf{Z}_{1:t-1}) &= \\ \frac{1}{N_p} \sum_{j=1}^{N_p} \delta(\mathbf{x}_{p,0:t-1}^j, \mathbf{g}_{0:t-1}^j, \mathbf{e}_{0:t-1}^j) \end{aligned} \quad (59)$$

By using this approximation, since all the distributions involved in (43) are known, an appropriate MCMC scheme can be used to draw from $p(\mathbf{x}_{p,0:t}, \mathbf{g}_{0:t}, \mathbf{e}_{0:t} | \mathbf{Z}_{1:t})$. The converged MCMC output are then extracted to give an empirical approximation of the posterior distribution of interest at time t , making possible the sequential inference. We call this scheme the MCMC-based particle algorithm.

At the m^{th} MCMC iteration, the following procedure is performed to obtain samples from $p(\mathbf{x}_{p,0:t}, \mathbf{g}_{0:t}, \mathbf{e}_{0:t} | \mathbf{Z}_{1:t})$:

- Make a joint draw for $\{\mathbf{x}_{p,0:t}^m, \mathbf{g}_{0:t}^m, \mathbf{e}_{0:t}^m\}$ using a Metropolis-Hastings step,
- Refine $\{\mathbf{x}_{p,t}^m, \mathbf{g}_t^m, \mathbf{e}_t^m\}$ using a series of Metropolis-Hastings-within-Gibbs steps.

These two steps are implemented in a mixture kernel so that the MCMC chain is irreducible and aperiodic [24]. At each iteration, the joint draw is performed with a probability ξ and the refinement step with probability $(1 - \xi)$.

Algorithm 1 Joint Proposal

- 1: Propose $\{\mathbf{x}_{p,0:t-1}^*, \mathbf{g}_{0:t-1}^*, \mathbf{e}_{0:t-1}^*\} \sim q(\mathbf{x}_{p,0:t-1}, \mathbf{g}_{0:t-1}, \mathbf{e}_{0:t-1})$
 - 2: Propose $\mathbf{g}_t^* \sim p(\mathbf{g}_t | \mathbf{x}_{p,t-1}^*, \mathbf{g}_{t-1}^*, \mathbf{e}_{t-1}^*)$
 - 3: Propose $\mathbf{e}_t^* \sim p(\mathbf{e}_t | \mathbf{e}_{t-1}^*)$
 - 4: Propose $\mathbf{x}_{p,t}^* \sim q(\mathbf{x}_{p,t} | \mathbf{x}_{p,0:t-1}^*, \mathbf{g}_{0:t}^*, \mathbf{e}_{0:t}^*)$
 - 5: With $\{\mathbf{x}_{p,0:t}^*, \mathbf{g}_{0:t}^*, \mathbf{e}_{0:t}^*\}$, calculate the acceptance ratio ρ_1 in Eq. (60)
 - 6: Sample a uniform random variable u from $\mathcal{U}(u|0, 1)$.
 - 7: **if** $u \leq \rho_1$ **then**
 - 8: $\{\mathbf{x}_{p,0:t}^m, \mathbf{g}_{0:t}^m, \mathbf{e}_{0:t}^m\} = \{\mathbf{x}_{p,0:t}^*, \mathbf{g}_{0:t}^*, \mathbf{e}_{0:t}^*\}$
 - 9: **else**
 - 10: $\{\mathbf{x}_{p,0:t}^m, \mathbf{g}_{0:t}^m, \mathbf{e}_{0:t}^m\} = \{\mathbf{x}_{p,0:t}^{m-1}, \mathbf{g}_{0:t}^{m-1}, \mathbf{e}_{0:t}^{m-1}\}$
 - 11: **end if**
-

$$\rho_1 = \min \left(1, \frac{\frac{p(\mathbf{Z}_t | \mathbf{x}_{p,t}^*, \mathbf{e}_t^*) p(\mathbf{x}_{p,t}^* | \mathbf{x}_{p,0:t-1}^*, \mathbf{e}_{0:t}^*, \mathbf{g}_{0:t}^*) \widehat{p}(\mathbf{x}_{p,0:t-1}^*, \mathbf{g}_{0:t-1}^*, \mathbf{e}_{0:t-1}^* | \mathbf{Z}_{1:t-1})}{q(\mathbf{x}_{p,t}^* | \mathbf{x}_{p,0:t-1}^*, \mathbf{g}_{0:t}^*, \mathbf{e}_{0:t}^*) q(\mathbf{x}_{p,0:t-1}^*, \mathbf{g}_{0:t-1}^*, \mathbf{e}_{0:t-1}^*)}}{\frac{p(\mathbf{Z}_t | \mathbf{x}_{p,t}^{m-1}, \mathbf{e}_t^{m-1}) p(\mathbf{x}_{p,t}^{m-1} | \mathbf{x}_{p,0:t-1}^{m-1}, \mathbf{e}_{0:t}^{m-1}, \mathbf{g}_{0:t}^{m-1}) \widehat{p}(\mathbf{x}_{p,0:t-1}^{m-1}, \mathbf{g}_{0:t-1}^{m-1}, \mathbf{e}_{0:t-1}^{m-1} | \mathbf{Z}_{1:t-1})}{q(\mathbf{x}_{p,t}^{m-1} | \mathbf{x}_{p,0:t-1}^{m-1}, \mathbf{g}_{0:t}^{m-1}, \mathbf{e}_{0:t}^{m-1}) q(\mathbf{x}_{p,0:t-1}^{m-1}, \mathbf{g}_{0:t-1}^{m-1}, \mathbf{e}_{0:t-1}^{m-1})}} \right) \quad (60)$$

Joint Proposal—To perform the joint draw, we use the scheme of Algorithm 1, which is a Metropolis-Hasting procedure. This algorithm starts with the sampling distribution of $\{\mathbf{x}_{p,0:t-1}, \mathbf{g}_{0:t-1}, \mathbf{e}_{0:t-1}\}$ from a proposal distribution $q(\mathbf{x}_{p,0:t-1}, \mathbf{g}_{0:t-1}, \mathbf{e}_{0:t-1})$. The easiest choice would be to make a uniform draw from the particle approximation $\widehat{p}(\mathbf{x}_{p,0:t-1}, \mathbf{g}_{0:t-1}, \mathbf{e}_{0:t-1} | \mathbf{Z}_{1:t-1})$ defined in (59). However to improve this step, we propose to use a weighted mixture of two distributions: the particle approximation of the posterior distribution at time $t-1$ and a distribution $\alpha(\mathbf{x}_{p,0:t-1}, \mathbf{g}_{0:t-1}, \mathbf{e}_{0:t-1})$ which takes into account the new received observations \mathbf{Z}_t and the particle set at time $t-1$, *i.e.*

$$\begin{aligned} q(\mathbf{x}_{p,0:t-1}, \mathbf{g}_{0:t-1}, \mathbf{e}_{0:t-1}) = & \\ & \sum_{j=1}^{N_p} P_a \alpha(\mathbf{x}_{p,0:t-1}^j, \mathbf{g}_{0:t-1}^j, \mathbf{e}_{0:t-1}^j) \\ & + \frac{1-P_a}{N_p} \delta(\mathbf{x}_{p,0:t-1}^j, \mathbf{g}_{0:t-1}^j, \mathbf{e}_{0:t-1}^j) \end{aligned} \quad (61)$$

where

$$\alpha(\mathbf{x}_{p,0:t-1}^j, \mathbf{g}_{0:t-1}^j, \mathbf{e}_{0:t-1}^j) = \frac{p(\mathbf{Z}_t | \widetilde{\mathbf{x}}_{p,t}^j, \widetilde{\mathbf{e}}_t^j)}{\sum_{i=1}^{N_p} p(\mathbf{Z}_t | \widetilde{\mathbf{x}}_{p,t}^i, \widetilde{\mathbf{e}}_t^i)} \quad (62)$$

with $\{\widetilde{\mathbf{e}}_t^j, \widetilde{\mathbf{g}}_t^j\} = \{\mathbf{e}_{t-1}^j, \mathbf{g}_{t-1}^j\}$ and $\widetilde{\mathbf{x}}_{p,t}^j = \mathbb{E}[\mathbf{x}_{p,t} | \mathbf{x}_{p,0:t-1}^j, \widetilde{\mathbf{e}}_t^j, \widetilde{\mathbf{g}}_t^j, \mathbf{e}_{0:t-1}^j, \mathbf{g}_{0:t-1}^j]$. The use of the distribution $\alpha(\mathbf{x}_{p,0:t-1}^j, \mathbf{g}_{0:t-1}^j, \mathbf{e}_{0:t-1}^j)$ is closely related to the auxiliary approach applied to particle filter [25]. This distribution leads to an improvement in the selection of a candidate in the existing particle set by taking into account the new observation. The presence of the original particle approximation in the proposal is used to ensure that a particle representing a good estimate of the previous state, $\{\mathbf{x}_{p,0:t-1}, \mathbf{g}_{0:t-1}, \mathbf{e}_{0:t-1}\}$, could be selected even if one or several actual targets are not detected in the new measurements set \mathbf{Z}_t .

After this first step, the group structure and the existence variable are sampled from their prior distribution, respectively given by Eq. (19) and Eq. (25). Then, position of the targets are drawn from the proposal $q(\mathbf{x}_{p,t} | \mathbf{x}_{p,0:t-1}^*, \mathbf{g}_{0:t}^*, \mathbf{e}_{0:t}^*)$ given by :

$$\begin{aligned} q(\mathbf{x}_{p,t} | \mathbf{x}_{p,0:t-1}^*, \mathbf{g}_{0:t}^*, \mathbf{e}_{0:t}^*) = & q_0(\mathbf{x}_{p,t}, \Upsilon_2^1) \\ & \times p(\mathbf{x}_{p,t}, \widetilde{\Upsilon} | \mathbf{x}_{p,0:t-1}^*, \mathbf{e}_{0:t}^*, \mathbf{g}_{0:t}^*) \end{aligned} \quad (63)$$

where $p(\mathbf{x}_{p,t}, \widetilde{\Upsilon} | \mathbf{x}_{p,0:t-1}^*, \mathbf{e}_{0:t}^*, \mathbf{g}_{0:t}^*)$, defined in Eq. (58), is obtained using the recursive equations of a pairwise Kalman filter associated to each particle. Compared to the prior distribution of $\mathbf{x}_{p,t,j}$ in Eq. (44), we only adopt a different proposal for the target birth. In order to improve the sample in this case, instead of sampling uniformly over the observation scene, we use a proposal based on measurements as we will expect the target to be more likely to appear in pixels that have measurements. This proposal is defined as follows :

$$q_0(\mathbf{x}_{p,t,j}) = \begin{cases} p_0(\mathbf{x}_{p,t,j}) & \text{if } N_{Obs}^t = 0 \\ P_I p_0(\mathbf{x}_{p,t,j}) & \text{otherwise} \\ + (1 - P_I) \phi(\mathbf{x}_{p,t,j} | \mathbf{Z}_{t-1:t}) \end{cases} \quad (64)$$

with

$$\begin{aligned} \phi(\mathbf{x}_{p,t,j} | \mathbf{Z}_{t-1:t}) = & \\ & \frac{1}{N_{Obs}^t} \sum_{m=1}^{N_{Obs}^t} \mathcal{U} \left(x_{t,j} | \beta_m^x \frac{L_x}{N_{pix}^x}, (\beta_m^x + 1) \frac{L_x}{N_{pix}^x} \right) \\ & \times \mathcal{U} \left(y_{t,j} | \beta_m^y \frac{L_y}{N_{pix}^y}, (\beta_m^y + 1) \frac{L_y}{N_{pix}^y} \right) \end{aligned} \quad (65)$$

where $\beta = \{\beta_m^x, \beta_m^y\}_{m=1}^{N_{Obs}^t}$ is the set of pixel coordinates of the observation scene where the measurements at time t are equal to 1 and where also the measurements at time $t-1$ are equal to 1 within one pixel of each other.

Group Structure	1	2	3	4	5	6	7	8	9	10	11	12	13	14	15
Target 1	1	1	1	1	1	1	1	1	1	1	1	1	1	1	1
Target 2	1	1	1	1	1	2	2	2	2	2	2	2	2	2	2
Target 3	1	1	2	2	2	1	1	1	2	2	2	3	3	3	3
Target 4	1	2	1	2	3	1	2	3	1	2	3	1	2	3	4

Table 2. Unique Group Representations for 4 Targets

After this sampling process, the acceptance ratio ρ_1 is computed, Eq. (60), and the candidate is accepted or not according to this one.

Refinement Step—To refine the estimate of $\{\mathbf{x}_{p,t}, \mathbf{g}_t, \mathbf{e}_t\}$, we propose to use a series of Metropolis-Hastings-within-Gibbs steps. We first start by sampling the group structure variable \mathbf{g}_t and then sampling each of the individual targets and their associated existence variables $\{\mathbf{x}_{p,t,i}, e_{t,i}\}$. For a target birth, the proposal based on measurements defined in (64) is also used. This step is summarised in Algorithm 2.

Algorithm 2 Refinement step

- 1: Propose $\mathbf{g}_t^* \sim p(\mathbf{g}_t | \mathbf{x}_{p,t-1}^{m-1}, \mathbf{g}_{t-1}^{m-1}, \mathbf{e}_{t-1}^{m-1})$
- 2: With \mathbf{g}_t^* , calculate the acceptance ratio

$$\rho_2 = \min \left(1, \frac{p(\mathbf{x}_{p,t}^{m-1} | \mathbf{x}_{p,0:t-1}^{m-1}, \mathbf{g}_{0:t-1}^{m-1}, \mathbf{g}_t^*, \mathbf{e}_{0:t}^{m-1})}{p(\mathbf{x}_{p,t}^{m-1} | \mathbf{x}_{p,0:t-1}^{m-1}, \mathbf{g}_{0:t}^{m-1}, \mathbf{e}_{0:t}^{m-1})} \right)$$

- 3: Sample a uniform random variable u from $\mathcal{U}(u|0,1)$ and set $\{\mathbf{g}_{0:t}^m\} = \{\mathbf{g}_{0:t-1}^{m-1}, \mathbf{g}_t^*\}$ if $u \leq \rho_2$, otherwise set $\{\mathbf{g}_{0:t}^m\} = \{\mathbf{g}_{0:t}^{m-1}\}$.
 - 4: Set $\{\mathbf{x}_{p,0:t}^m, \mathbf{e}_{0:t}^m\} = \{\mathbf{x}_{p,0:t}^{m-1}, \mathbf{e}_{0:t}^{m-1}\}$
 - 5: **for** each target i **do**
 - 6: Propose $e_{t,i}^* \sim p(e_{t,i} | e_{t-1,i}^m)$
 - 7: Propose $\mathbf{x}_{p,t,i}^* \sim q(\mathbf{x}_{p,t,i} | \mathbf{x}_{p,0:t-1}^m, \mathbf{x}_{p,t,\setminus i}^m, \mathbf{g}_{0:t}^m, \mathbf{e}_{0:t-1}^m, \mathbf{e}_{t,\setminus i}^m, e_{t,i}^*)$
 - 8: With $\{e_{t,i}^*, \mathbf{x}_{p,t,i}^*\}$, calculate the acceptance ratio ρ_3 in Eq. (66)
 - 9: Sample a uniform random variable u from $\mathcal{U}(u|0,1)$ and set $\{e_{t,i}^m, \mathbf{x}_{p,t,i}^m\} = \{e_{t,i}^*, \mathbf{x}_{p,t,i}^*\}$ if $u \leq \rho_3$, otherwise set $\{e_{t,i}^m, \mathbf{x}_{p,t,i}^m\} = \{e_{t,i}^{m-1}, \mathbf{x}_{p,t,i}^{m-1}\}$.
 - 10: **end for**
-

$$\rho_3 = \min \left(1, \frac{\frac{p(\mathbf{Z}_t | \mathbf{x}_{p,t,\setminus i}^m, \mathbf{x}_{p,t,i}^*, \mathbf{e}_{t,\setminus i}^m, e_{t,i}^*) p(\mathbf{x}_{p,t,\setminus i}^m | \mathbf{x}_{p,0:t-1}^m, \mathbf{x}_{p,t,i}^* | \mathbf{x}_{p,0:t-1}^m, \mathbf{g}_{0:t}^m, \mathbf{e}_{0:t-1}^m, \mathbf{e}_{t,\setminus i}^m, e_{t,i}^*)}{q(\mathbf{x}_{p,t,i}^* | \mathbf{x}_{p,0:t-1}^m, \mathbf{x}_{p,t,\setminus i}^m, \mathbf{g}_{0:t}^m, \mathbf{e}_{0:t-1}^m, \mathbf{e}_{t,\setminus i}^m, e_{t,i}^*)}}{\frac{p(\mathbf{Z}_t | \mathbf{x}_{p,t,\setminus i}^m, \mathbf{e}_{t,i}^m) p(\mathbf{x}_{p,t,\setminus i}^m | \mathbf{x}_{p,0:t-1}^m, \mathbf{g}_{0:t}^m, \mathbf{e}_{0:t}^m)}{q(\mathbf{x}_{p,t,i}^m | \mathbf{x}_{p,0:t-1}^m, \mathbf{x}_{p,t,\setminus i}^m, \mathbf{g}_{0:t}^m, \mathbf{e}_{0:t}^m)}} \right) \quad (66)$$

5. NUMERICAL RESULTS

A single discretised sensor model is used which scans a fixed rectangular region of 100 by 100 pixels, where each pixel is 50m by 50m. Thresholded measurements are used with $P_{d,1} = 0.7$ and a false alarm probability for each pixel of $P_{fa} = 0.002$ (*i.e.* SNR= 17 dB). The sensor returns a set of observations every 5s.

We use the group dynamic model, Eq. (13), to generate a set of tracks of four targets shown in Figure 3. This scenario consists of 2 groups of 2 targets moving towards each other from time step 1 to 45, and then merged to form a combined group from time step 46 to 110. The parameters used to generate the motion of the group is the same as the simulations in previous section shown in Table 1. For 4 targets, Table 2 lists all the possible group combinations.

The MCMC-based particle algorithm is used to detect and track targets in the scenario described above. A Monte Carlo run of 40 sets of the observations of the 4 targets are generated. For each run, all the particles are initialised as inactive in order to allow the algorithm to detect all targets unaided. At each time step, 24000 MCMC iterations are performed with burn-in of 1000 iterations. At each MCMC iteration, the joint proposal is performed with a probability $\xi = 0.75$. The particle approximation

of $p(\mathbf{x}_{p,0:t}, \mathbf{g}_{0:t}, \mathbf{e}_{0:t} | \mathbf{Z}_{1:t})$ is obtained using $N_p = 4000$ particles by storing every 6th sample (thinning) after the initial burn-in iterations. P_{NC} , P_Q , $\{P_B; P_D\}$, P_a and P_I respectively involved in Eq. (19), (23), (25), (61) and (64) are set to 0.6, 0.05, $\{0.2; 0.05\}$, 0.5 and 10^{-2} .

The estimated tracks for a single run are shown in Fig. 4. The MCMC-Particles Algorithm has successfully detected and tracked the 4 targets. The ellipse shows the mode of the group configuration and the number indicates the number of targets in the group. The proposed algorithm is clearly able to infer the correct group structure. This can be also be seen in Figure 5, which shows the time evolution of the group structure probability obtained by the algorithm. The group structure change from $[1\ 1\ 2\ 2]^T$ to $[1\ 1\ 1\ 1]^T$ can be clearly identified in this figure.

Finally, Figure 6 shows the mean of the existence variables over the 40 Monte Carlo runs. From this figure, we can see that the proposed algorithm is able to detect consistently and rapidly that there are 4 targets in the observation scene.

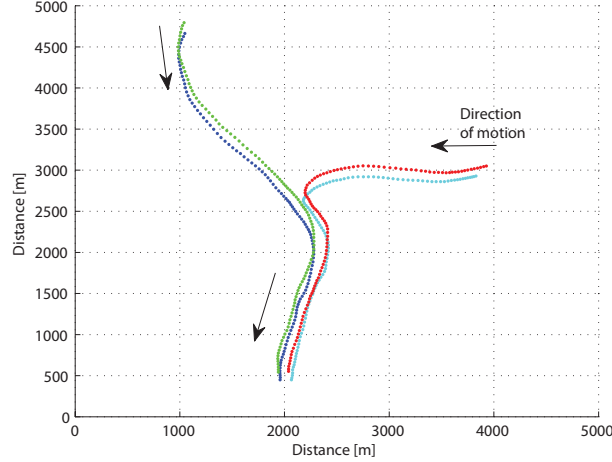


Figure 3. Ground truth of the group merging simulation scenario for two groups of two targets.

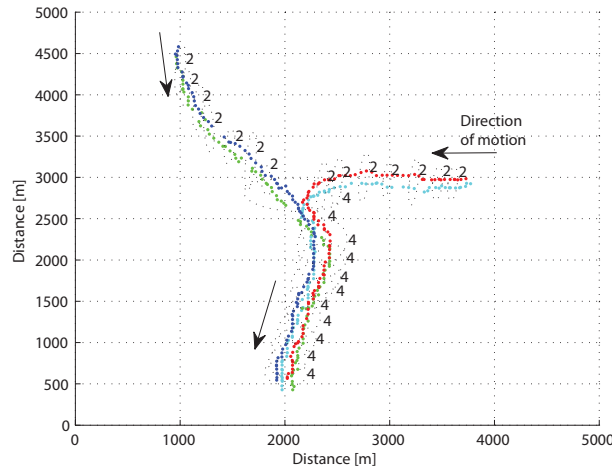


Figure 4. Tracking results for a single run of the MCMC-based particle algorithm (the ellipse shows the mode of the group configuration, labelled with the number of objects detected in the group).

6. CONCLUSIONS

In this paper, we have focused our study on the problem of tracking coordinated formations of targets using a group dynamical model with a virtual leader. A MCMC-based particle algorithm is proposed to approximate the filtering distribution of the high dimensional state of interest. The proposed algorithm is then efficiently designed with the auxiliary idea used traditionally in particle filtering and with the marginalisation of both the target velocity and the virtual leader kinematics using pairwise Kalman filters. Numerical simulations clearly show that this algorithm is able to detect targets within groups, as well as infer the correct group structure and the number of targets over time.

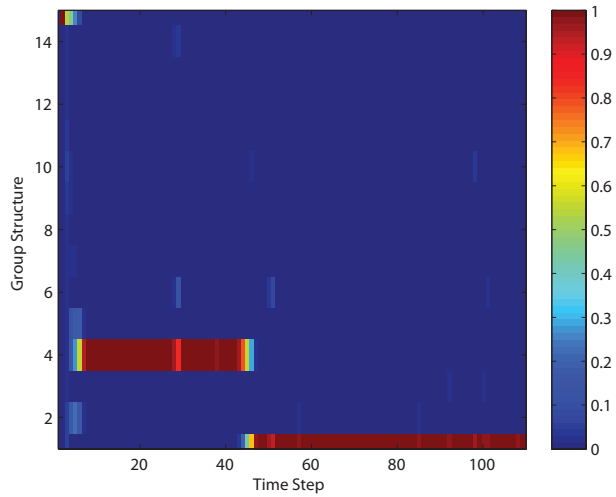


Figure 5. Group structure probability over time obtained with the proposed algorithm.

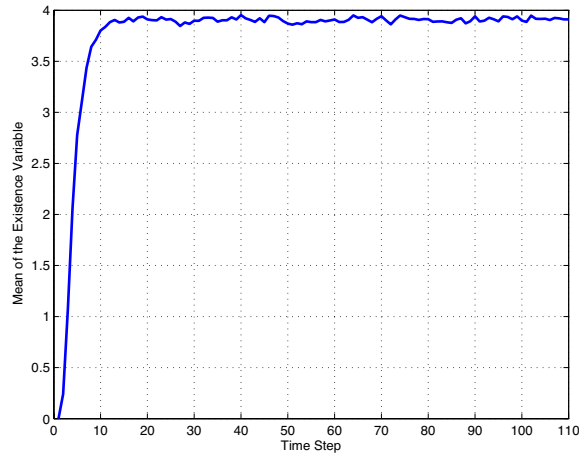


Figure 6. Mean of the existence variables over 40 runs of the MCMC-based particle algorithm.

ACKNOWLEDGMENTS

This research was sponsored by the Data and Information Fusion Defence Technology Centre, UK, under the Tracking Cluster. The authors thank these parties for funding this work.

REFERENCES

- [1] N. J. Gordon, D. J. Salmond, and D. Fisher, “Bayesian Target Tracking After Group Pattern Distortion,” in *Signal and Data Processing of Small Targets, SPIE*, 1997, pp. 238–248.
- [2] K. Gilholm and D. Salmond, “Spatial Distribution Model for Tracking Extended Objects,” *IEE Proceedings on Radar, Sonar and Navigation*, Oct. 2005.
- [3] K. Gilholm, S. Godsill, S. Maskell, and D. Salmond, “Poisson Models for Extended Target and Group Tracking,” *SPIE Conference : Signal and Data Processing of Small Targets, Proceedings of*, Aug. 2005.
- [4] W. Ng, J. Li, and S. J. Godsill, “Multiple and Extended Object Tracking with Poisson Spatial Process and Variable Rate Filters,” in *First IEEE International Workshop on Computational Advances in Multi-Sensor Adaptive Processing*, 2005.
- [5] R. P. S. Mahler, “An Extended First-Order Bayes Filter for Force Aggregation,” in *SPIE*, vol. 4728, 2002, pp. 196–207.
- [6] R. P. S. Mahler and T. Zajic, “Bulk Multitarget Tracking using a First-Order Multitarget Moment Filter,” in *SPIE*, vol. 4729, 2002, pp. 175–186.

- [7] D. Clark and S. J. Godsill, "Group Target Tracking with the Gaussian Mixture Probability Hypothesis Density Filter," in *Third International Conference on Intelligent Sensors, Sensor Networks and Information Processing*, Dec. 2007.
- [8] S. K. Pang, J. Li, and S. J. Godsill, "Models and Algorithms for Detection and Tracking of Coordinated Groups," in *IEEE Aerospace Conference*, Mar. 2008, pp. 1–17.
- [9] B. Ristic, S. Arulampalam, and N. Gordon, *Beyond the Kalman filter - Particle Filters for Tracking Applications*. 685 Canton Street, Norwood, MA 02062: Artech House, 2004.
- [10] R. P. S. Mahler, *Statistical Multisource-Multitarget Information Fusions*. 685 Canton Street, Norwood, MA 02062: Artech House, 2007.
- [11] Z. Khan, T. Blach, and F. Dellaert, "MCMC-based Particle Filtering for Tracking a Variable Number of Interacting Targets," *IEEE Transactions on Pattern Analysis and Machine Intelligence*, vol. 27, pp. 1805–1819, Nov. 2005.
- [12] S. K. Pang, J. Li, and S. Godsill, "Models and Algorithms for Detection and Tracking of Coordinated Groups," in *5th International Symposium on Image and Signal Processing and Analysis*, Nov. 2007.
- [13] S. Sarkka, "Recursive Bayesian Inference on Stochastic Differential Equations," Ph.D. dissertation, Helsinki University of Technology, Department of Electrical and Communications Engineering, 2006.
- [14] R. F. Stengel, *Optimal Control and Estimation*. Dover Publications, Inc, 1994.
- [15] J. Vermaak, S. Maskell, M. Briers, and P. Perez, "A Unifying Framework for Multi-Target Tracking and Existence," in *8th International Conference on Information Fusion*, vol. 1, Jul. 2005, pp. 25–28.
- [16] C. Kreucher, M. Morelande, K. Kastella, and A. O. H. III, "Particle Filtering for Multitarget Detection and Tracking," *IEEE Transactions on Aerospace and Electronic Systems*, vol. 41, pp. 1396–1414, Oct. 2005.
- [17] Y. Boers and H. Diressen, "Particle Filter Based Track Before Detect Algorithms," in *SPIE Conf. on Signal and Data Processing of Small Targets*, vol. 5204, Aug. 2003, pp. 25–28.
- [18] M. Rutten, N. Gordon, and S. Maskell, "Particle-Based Track Before Detect in Rayleigh Noise," in *SPIE Conf. on Signal and Data Processing of Small Targets*, vol. 5204, 2004.
- [19] C. Berzuini, N. G. Best, W. R. Gilks, and C. Larizza, "Dynamic Conditional Independence Models and Markov Chain Monte Carlo Methods," *Journal of the American Statistical Association*, vol. 440, pp. 1403–1412, Dec. 1997.
- [20] A. Golightly and D. J. Wilkinson, "Bayesian Sequential Inference for Nonlinear Multivariate Diffusions," *Statistics and Computing*, pp. 323–338, Aug. 2006.
- [21] W. R. Gilks and C. Berzuini, "Following a Moving Target-Monte Carlo Inference for Dynamic Bayesian Models," *Journal of the Royal Statistical Society. series B (Statistical Methodology)*, vol. 63, pp. 127–146, 2001.
- [22] W. Pieczynski, "Pairwise Markov Chains," *IEEE Transactions on Pattern Analysis and Machine Intelligence*, vol. 25, no. 5, pp. 634–639, 2003.
- [23] W. Pieczynski and F. Desbouvries, "Kalman Filtering using Pairwise Gaussian Models," in *IEEE International Conference on Acoustics, Speech and Signal Processing (ICASSP'03)*, vol. 6, Apr. 2003, pp. 57–60.
- [24] L. Tierney, "Markov Chains for Exploring Posterior Distributions," *Annals of Statistics*, vol. 22, pp. 1701–1786, 1994.
- [25] M. Pitt, N. Shephard, and N. C. Oxford, "Filtering Via Simulation: Auxiliary Particle Filters." *Journal of the American Statistical Association*, vol. 94, no. 446, pp. 590–591, 1999.

BIOGRAPHY



François Septier received the Engineer degree in electrical engineering and signal processing in 2004 from TELECOM Lille 1, France, and the M.S. degree in digital communications and a Ph.D. in Electrical Engineering both from the University of Valenciennes, France, in 2004 and 2008 respectively. He is currently a Research Associate in the Signal Processing and Communications Laboratory, Cambridge University Engineering Department, UK. His research focuses on Monte-Carlo statistical methods for digital communications, multitarget tracking and source term estimation.



Sze Kim Pang received the M.Eng. degree in electrical and electronic engineering from Imperial College, UK in 1997. Since 1999, he has been with DSO National Laboratories, Singapore, where he is now a Senior Member of Technical Staff. His work covers research and development in statistical and array signal processing. Currently, he is pursuing a Ph.D. Degree in the Signal Processing and Communications Laboratory, Cambridge University Engineering Department. His research focuses on multitarget detection and tracking using Bayesian statistical signal processing.



Simon J. Godsill is Professor in Statistical Signal Processing in the Engineering Department of Cambridge University. He is an Associate Editor for IEEE Trans. Signal Processing and the journal Bayesian Analysis, and is a member of IEEE Signal Processing Theory and Methods Committee. He has research interests in Bayesian and statistical methods for signal processing, Monte Carlo algorithms for Bayesian problems, modeling and enhancement of audio and musical signals, source separation, tracking and genomic signal processing. He has published extensively in journals, books and conferences. He has co-edited in 2002 a special issue of IEEE Trans. Signal Processing on Monte Carlo Methods in Signal Processing and a recent special issue of the Journal of Applied Signal Processing, and organised many conference sessions

on related themes.



Avishy Carmi received his Ph.D. in aerospace engineering from the Technion - Israel institute of technology in 2008. He is currently a Research Associate in the Signal Processing and Communications Laboratory at the department of engineering University of Cambridge, UK. His primary research focuses on estimation theory, Monte Carlo statistical methods and optimisation.